Turkish Journal of Electrical Engineering & Computer Sciences

http://journals.tubitak.gov.tr/elektrik/

Research Article

Turk J Elec Eng & Comp Sci
(2017) 25: 4496 – 4509

doi:10.3906/elk-1703-170

Method of singular integral equations in diffraction by semi-infinite grating: H-polarization case

Mstislav KALIBERDA[1,*], **Leonid LYTVYNENKO**[2], **Sergey POGARSKY**[1]
[1]Department of Radiophysics, V. Karazin National University of Kharkiv, Kharkiv, Ukraine
[2]Institute of Radio Astronomy of the National Academy of Sciences of Ukraine, Kharkiv, Ukraine

Received: 14.03.2017 • **Accepted/Published Online:** 25.09.2017 • **Final Version:** 03.12.2017

Abstract: Diffraction of the H-polarized electromagnetic wave by a semi-infinite strip grating is considered. The scattered field is represented as a superposition of the field induced by the currents on the strips of an infinite periodic grating and the field induced by the correction current excited due to end of the grating. Singular integral equations with additional conditions for infinite and semi-infinite periodic gratings are obtained. The current on the strips and spectral function of scattered field are expressed in terms of the solution of these equations. Numerical results for the near and far fields distribution are represented.

Key words: Semi-infinite grating, singular integral equation, diffraction

1. Introduction

Periodic strip gratings have a variety of applications in microwave engineering and optics. Often, actual gratings consist of a large number of identical elements. To simulate such objects, the model of infinite periodic grating (IPG) can be used. However, it does not take into account the influence of the end of a real finite grating. Effects caused by the truncation can be described by the semi-infinite gratings (SIG) and these results can be used to analyze finite arrays [1–4]. The semi-infinite periodic structures are infinitely extended in one direction but they are bounded in the other one. Thus, Floquet's theorem cannot be applied here. The methods of analysis of finite gratings also cannot be applied directly to the SIG because of their infinite size.

In [5,6], the SIG of the cylinder scatterers is considered. The cylinder radius is small as against the wavelength. The correction for the current on the first four wires is obtained. The problem is reduced to the heterogeneous Gilbert one and is solved using the variational approach. In [7] and [8], a similar problem is analyzed using the discrete Wiener–Hopf method. The application of the Wiener–Hopf technique to the SIG of cylindrical and spherical scatterers is also described in [9–11]. In [12], the Wiener–Hopf technique is applied to the plane SIG of strips. The E-polarization case is considered. The current on the strips is represented as a superposition of the current on the IPG and the correction current. The single-shape basic function approximation for the correction current is used. The comparison with the method of moments (MoM) with the same basic functions choice is given. Strip width is much smaller than the wavelength so as the single basis function approximation is justifiable.

In [1], the current on the strips is also represented as a sum of the current on the IPG and the correction

*Correspondence: kaliberdame@yandex.ru

current. The electric field integral equations in the E-polarization case are solved in the assumption that the phase of the current on the strips is constant over the strip, but the amplitude has singularities at the strip edges. In this solution, the strip width should be much smaller than the wavelength. In a subsequent paper [2], the solution is obtained with no restriction on the strip width and period. The MoM is used with the pulse functions taken as the bases functions and the delta functions taken as the weighting functions. Numerical results are given for the resonance case when the strip width is equal to the wavelength.

In [13], the diffraction problem by the SIG is reduced to the so-called canonical one, which is solved by the Sommerfeld–Maliuzhinets method. The approximate boundary condition technique is used. The solution is obtained in the assumption of the small period as compared to the wavelength.

In [14], SIG of strips on the grounded slab excited by the surface mode is considered. The current on the strips of the IPG on the grounded slab is obtained by the MoM. It is used to find the approximation of the solution for the SIG.

Specific translation symmetry of the semi-infinite structures meaning that no SIG properties change with its last element removed is used in [15–19]. Scattered field is expressed with the use of the reflection operator obtained by the operator method from the nonlinear operator equation. In [20], different approaches to diffraction by one-dimensional semi-infinite array are discussed.

In the E-polarization case, when representing fields in the form of single-layered potentials, the kernel function of the electric field integral equations has logarithmic singularity. However, in the H-polarization case, the kernel function has hyper-singularity. Several papers propose the regularization procedure connected to the exclusion of singularities. As a result, the second-kind equation of the Fredholm type can be obtained [21,22]. In [23,24], a method of analytical preconditioning is discussed. Papers propose the Galerkin-projection technique with the set of orthogonal eigenfunctions of the singular part of the integral operator as a basis, which results in a regularized discretization scheme. It combines both regularization and discretization in one single procedure. In [25], a new analytically regularizing procedure, based on Helmholtz decomposition and the Galerkin method, employed to analyze the electromagnetic scattering by a zero-thickness perfectly electrical conducting circular disk is presented. In [26], the MoM is used. The derivatives in the electric field integral equations are evaluated using the finite-difference scheme, and then sinc functions are used to approximate the unknown current distribution on strips. Other papers give the Nystrom-type algorithm [27–33]. It proposes direct discretization of the singular or hyper-singular integral equations. The integrand is exchanged by the polynomials and then the Gauss–Chebyshev quadrature formulas of interpolation type, which take into account the edge behavior of the current on the scatterers, are applied.

In recent years, the Nystrom-type algorithms have attracted attention and are developed for analysis of diffraction by the IPG or finite number of thin strips-like scatterers. In this paper, we are going to extend one of such algorithms for the infinite but not ideally periodic grating. Here we are going to consider the SIG. We represent the scattered field in the spectral-domain as a sum of the field of the IPG and unknown correction field excited due to the end of the grating. The singular integral equations (SIE) obtained relatively to derivative of the x-component of the magnetic field on the strips are solved by using the Nystrom-type method of discrete singularities (MDS) [31–33]. It should be mentioned that the x-component of the magnetic field equals up to a factor to the current distribution on the strips. MDS being an efficient method of discretization of SIE has theoretically guarantied and controlled convergence. It is not connected with the appropriate choice of the basic-functions as in the MoM. As it was mentioned in [32], in contrast with other Nystrom-type algorithms where a segment of integration is divided into parts, and the specific interpolation scheme, which takes into

account the current singularity, is applied only to the edge segments [29], here a quadrature rule is applied to the whole strip and takes into account edge singularity. In order to study effects caused by the truncation of the real finite array, numerical calculations are carried out for current and near field distributions and diffraction patterns.

2. Solution of the problem

Consider a SIG placed in the $z = 0$ plane. The middle of the strip with number $n = 0$ coincides with the right-side Cartesian coordinate system. The strip width is $2\ d$ and period is l. Strips are infinite along the x-axis. The structure geometry is shown in Figure 1. The time factor is $\exp(-i\omega t)$. Suppose that an H-polarized plane wave is incident on the grating

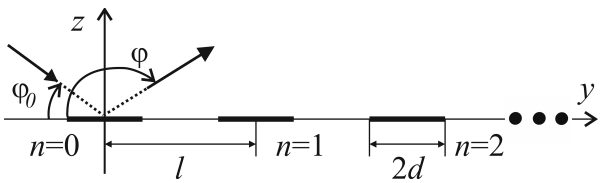

Figure 1. Structure geometry.

$$H_x^i(y,z) = \exp\left(ik(y\cos\phi_0 - z\sin\phi_0)\right),$$

where k is the wavenumber and ϕ_0 is the incidence angle to the y-axis. The scattered field we represent as the superposition of the field induced by the currents on the strips of the IPG, $H_x^{s,inf}(y,z)$, and the field induced by the correction current excited due to end of the SIG, $H_x^{s,c}(y,z)$,

$$H_x^s(y,z) = H_x^{s,inf}(y,z) + H_x^{s,c}(y,z). \tag{1}$$

Field $H_x^{s,inf}(y,z)$ can be represented as a sum of the fields excited by the currents on the strips of the IPG. Field of the mth strip of the IPG we represent in the form of the double-layered potential

$$\frac{i}{4}\int\limits_{-d}^{d}\mu_m^{\infty}(y'+lm)\frac{\partial}{\partial z'}H_0^{(1)}\left(k\sqrt{(y-y'-lm)^2+(z-z')^2}\right)dy'.$$

Then

$$H_x^{s,inf}(y,z) = \frac{i}{4}\sum_{m=0}^{\infty}\int\limits_{-d}^{d}\mu_m^{\infty}(y'+lm)\frac{\partial}{\partial z'}H_0^{(1)}\left(k\sqrt{(y-y'-lm)^2+(z-z')^2}\right)dy', \quad z' = \ 0, \tag{2}$$

where $\mu_m^{\infty}(y'+lm)$ is equal up to a factor to the current density on the strips of the IPG. Summation is performed over all strips of the SIG, $m = \ 0, 1, \ldots$. Correction field $H_x^{s,c}(y,z)$ we represent in the form of the Fourier integral

$$H_x^{s,c}(y,z) = \int\limits_{-\infty}^{\infty} c(\xi)\exp\left(ik(\xi y + \gamma(\xi)z)\right)d\xi, \quad z > \ 0, \tag{3}$$

$$H_x^{s,c}(y,z) = -\int\limits_{-\infty}^{\infty} c(\xi)\exp\left(ik(\xi y - \gamma(\xi)z)\right)d\xi, \quad z < 0,$$

where $c(\xi)$ is the spectral function, $\gamma(\xi) = \sqrt{1-\xi^2}$, $Re\gamma \geq 0$, $Im\gamma \geq 0$.

Denote the set of strips as $L = \bigcup\limits_{m=0}^{\infty}(-d+lm;\, d+lm)$. By applying boundary and continuity conditions, the dual integral equations can be obtained

$$\int\limits_{-\infty}^{\infty} c(\xi)\exp(ik\xi y)d\xi = 0, \quad y \notin L, \tag{4}$$

$$\int\limits_{-\infty}^{\infty} c(\xi)\gamma(\xi)\exp(ik\xi y)d\xi = \frac{i}{k}\left(\frac{\partial}{\partial z}H_x^i(y,0) + \frac{\partial}{\partial z}H_x^{s,inf}(y,0)\right) = g(y), \quad y \in L. \tag{5}$$

2.1. Singular integral equation

In this section, we are going to reduce (4) and (5) to the singular integral equation relatively unknown derivative of the correction current density on the strips. Introduce the Fourier transform of the unknown spectral function of the correction field $c(\xi)$

$$U(y) = \int\limits_{-\infty}^{\infty} c(\xi)\exp(iky\xi)d\xi. \tag{6}$$

Function $U(y)$ is up to a constant factor the correction current on the strips, $U(y) = 0$ when $y \notin L$. The derivative of $U(y)$ is denoted as [31,33]

$$U'(y) = F(y) = \int\limits_{-\infty}^{\infty} ik\xi c(\xi)\exp(iky\xi)d\xi, \tag{7}$$

and $F(y) = 0$ when $y \notin L$. Then using the inverse Fourier transformation obtain

$$c(\xi) = \frac{1}{2\,\pi\, i\xi}\int\limits_{L} F(y)\left(\exp(iky\xi) - 1\right)dy. \tag{8}$$

From (5) and (7) it follows that

$$\frac{1}{\pi ik}PV\int\limits_{-\infty}^{\infty}\frac{F(\xi)}{\xi - y}d\xi - \int\limits_{-\infty}^{\infty} c(\xi)\exp(iky\xi)\left(i\,|\xi| - \gamma(\xi)\right)d\xi = g(y). \tag{9}$$

The Hilbert transform $\frac{1}{\pi}PV\int\limits_{-\infty}^{\infty}\frac{\exp(ik\xi\zeta)}{\xi - y}d\xi = isgn(k\zeta)\exp(ik\zeta y)$ was applied here. The first integral in (9) is understood in the sense of Cauchy principal value integral.

Using (8), from (9) we have SIE

$$\frac{1}{\pi}PV\int\limits_L \frac{F(\xi)}{\xi-y}d\xi+\frac{1}{\pi}\int\limits_L K(y,\xi)F(\xi)d\xi=ikg(y),\quad y\in L. \tag{10}$$

The kernel function $K(y,\xi)$ is

$$K(y,\xi)=k\int\limits_0^\infty \frac{\sin(k\zeta(y-\xi))}{\zeta}(\zeta+i\gamma(\zeta))d\zeta.$$

The integral in $K(y,\xi)$ converges as $1/\zeta^2$, when $\zeta\to\infty$. Using the asymptotic for $\gamma(\zeta)\sim i\zeta-i/(2\,\zeta)-i/(8\,\zeta^3)$, when $\zeta\to\infty$, and expression for sine integral one may increase the convergence rate. In our calculations the integral converges as $1/\zeta^6$, when $\zeta\to\infty$. For details, see e.g. [30].

The additional conditions, which are necessary to choose a unique solution of (9), follow from (4)

$$\frac{1}{\pi}\int\limits_{-d}^{d} F(\xi+lm)d\xi=\ 0,\quad m=\ \pm1,\ \pm2,\ ....\tag{11}$$

Note that SIE (10) with additional conditions (11) is fully equivalent to the original boundary-value problem. To solve (10) and obtain total scattered field (1), we should evaluate $H_x^{s,inf}(y,z)$.

2.2. Field $H_x^{s,inf}(y,z)$

In spectral domain field scattered by the IPG is expressed using the Fourier series

$$H_x^{inf}(y,z)=\sum_{n=-\infty}^{\infty} a_n\exp\left(ik(\zeta_n y+\gamma_n z)\right),\quad z>\ 0,$$

$$H_x^{inf}(y,z)=-\sum_{n=-\infty}^{\infty} a_n\exp\left(ik(\zeta_n y-\gamma_n z)\right),\quad z<\ 0,$$

where $\zeta_n=\frac{2\pi n}{kl}+\cos\phi_0$, $\gamma_n=\sqrt{1-\left(\frac{2\pi n}{kl}+\cos\phi_0\right)^2}$, $Re\gamma_n\geq\ 0$, $Im\gamma_n\geq\ 0$. Then

$$\mu_m^\infty(y)=\begin{cases} 2\sum\limits_{n=-\infty}^{\infty} a_n\exp(ik\zeta_n y), & |y-ml|\leq d,\\ 0, & |y-ml|>d.\end{cases}\tag{12}$$

By substituting (12) into (2) obtain the expression for $H_x^{s,inf}(y,z)$ and for the right-hand side of (10)

$$H_x^{s,inf}(y,z)=\frac{i}{2}\sum_{m=0}^{\infty}\int\limits_{-d}^{d}\sum_{n=-\infty}^{\infty} a_n\exp(ik\zeta_n(y'+lm))\frac{\partial}{\partial z'}H_0^{(1)}\left(k\sqrt{(y-y'-lm)^2+(z-z')^2}\right)dy',z'=\ 0,$$

$$g(y)=\frac{1}{2}\sum_{m=-\infty}^{-1}\int\limits_{-d}^{d}\sum_{n=-\infty}^{\infty} a_n\exp\left(ik\zeta_n(y'+lm)\right)\frac{H_1^{(1)}\left(k\left|y-y'-lm\right|\right)}{|y-y'-lm|}dy'.$$

Notice that integrands in $g(y)$ do not contain singularities when $y \in L$.

Unknown Fourier amplitudes a_n can be obtained from the dual summatory equations

$$\sum_{n=-\infty}^{\infty} a_n \exp\left(i\frac{2\pi n}{l}y\right) = 0, \text{ for slots,} \tag{13}$$

$$\sum_{n=-\infty}^{\infty} a_n\gamma_n \exp\left(i\frac{2\pi n}{l}y\right) = \gamma_0, \text{ for strips.} \tag{14}$$

Equations (13) and (14) can be reduced to the singular integral equation with additional condition similar to (10) and (11) [31,33]

$$\frac{1}{\pi}PV\int_{-\delta}^{\delta}\frac{F(\xi)}{\xi-\psi}d\xi + \frac{1}{\pi}\int_{-\delta}^{\delta}K_{2\pi}(\psi,\xi)F(\xi)d\xi = i\kappa\gamma_0, \quad |\psi| < \delta,$$

$$\frac{1}{\pi}\int_{-\delta}^{\delta}F(\xi)d\xi = 0,$$

where

$$a_n = \frac{1}{2\pi i n}\int_{-\delta}^{\delta}F(\xi)\exp(-in\xi)d\xi, \quad n \neq 0,$$

$$a_0 = -\frac{1}{\pi}\int_{-\delta}^{\delta}\frac{\xi}{2}F(\xi)d\xi,$$

$\psi = 2\pi y/l \quad \delta = 2\pi d/l, \quad \kappa = kl/(2\pi)$ are nondimensional quantities. The kernel function is

$$K_{2\pi}(\psi,\xi) = -\frac{\kappa}{2}\sum_{\substack{n=-\infty\\ n\neq 0}}^{\infty}\left(\frac{i|n|}{\kappa}-\gamma_n\right)\frac{\exp\left(in(\psi-\xi)\right)}{n} + +i\gamma_0\kappa\frac{\psi-\xi}{2} + \left(\frac{1}{\psi-\xi} - \frac{1}{2}ctg\left(\frac{\psi-\xi}{2}\right)\right).$$

Using the asymptotic for $\gamma_n \sim \frac{i|n|}{\kappa} - \frac{i|n|}{n}\sin\alpha$, when $n \to \infty$, one may obtain expression for $K_{2\pi}(\psi,\xi)$, which converges as $1/n^3$, when $n \to \infty$ (see [30]).

2.3. Method of discrete singularities

Notice that according to the edge condition function $F(\xi)$ have root type singularities,

$$F(t_{q,m}^{(M)}) = \frac{u(t_{q,m}^{(M)})}{\sqrt{\left(t_{q,m}^{(M)} - (-d+lm)\right)\left((d+lm) - t_{q,m}^{(M)}\right)}}.$$

In (10) and (11) exchange the integrands by the polynomials and then apply the Gauss–Chebyshev quadrature formulas of interpolation type for the weight-function $1/\sqrt{1-x^2}$ with nodes taken at the zeros of the Chebyshev

polynomials of the first kind. Represent integral over L as a sum of integrals over every segment $(-d+l\cdot n;\ d+l\cdot n)$, $\int\limits_L(\cdots)=\sum\limits_{n=0}^{\infty}\int\limits_{-d+l\cdot n}^{d+l\cdot n}(\cdots)$. Then using the MDS the following system of linear algebraic equations can be obtained from (10) and (11) [30–33]

$$\frac{1}{M}\sum_{n=0}^{\infty}\left(\sum_{q=1}^{M}\frac{u(t_{q,n}^{(M)})}{t_{q,n}^{(M)}-\hat{t}_{l,m}^{(M-1)}}+\sum_{q=1}^{M}K(\hat{t}_{l,m}^{(M-1)},t_{q,n}^{(M)})u(t_{q,n}^{(M)})\right)=ikg(\hat{t}_{l,m}^{(M-1)}), \tag{15}$$

$$\frac{1}{M}\sum_{q=1}^{M}u(t_{q,m}^{(M)})=0,\quad l=1,2,...,M-1,\quad m=0,1,..., \tag{16}$$

where $t_{q,m}^{(M)}\in(-d+lm;\ d+lm)$ are the zeros of the Chebyshev polynomials of the first kind on every segment, $q=1,2,...M$; $\hat{t}_{q,m}^{(M-1)}\in(-d+lm;\ d+lm)$ are the so-called collocation points, which are zeros of the Chebyshev polynomials of the second kind on every segment, and M is the number of nodes on every segment. After solving (15) and (16) the values of $F(\xi)$ in the interpolation nodes can be obtained. The values of $F(\xi)$ in other points, $\xi\in(-\infty;\infty)$, can be obtained from the corresponding interpolation polynomial.

3. Field representation

3.1. Far field

In the far field region, the scattered field can be represented as a superposition of plane waves (Floquet's modes) $H_x^p(\rho,\phi)$ and a cylindrical wave. Function $H_x^p(\rho,\phi)$ obviously does not decrease if $k\rho\to\infty$, where $\rho=\sqrt{y^2+z^2}$ is distance. The amplitude and direction of propagation of plane waves coincide with those of IPG [7]. However, plane waves exist only in the domain $\phi>w_q$, where w_q is propagation angle of the qth plane wave relative to the y-axis. Line $\phi=w_q$ acts as a shadow boundary. Near the shadow boundary, the first order solution of the saddle point method fails since the poles and saddle point are close to each other. Then the field in the transition region near $\phi=w_q$ is represented in terms of the Gauss error function $H_x^{erfc}(\rho,\phi)$.

Using the integral representation of the Hankel function for $H_x^{s,inf}(\rho,\phi)$ obtain

$$\begin{aligned}H_x^{s,inf}(y,z) &= \frac{ksgnz}{2\pi}\int\limits_{-\infty}^{\infty}\frac{\exp(ik\xi y+ik|z|\gamma(\xi))}{1-\exp\left(ikl(\cos\phi_0-\xi)\right)}\int\limits_{-d}^{d}\sum_{n=-\infty}^{\infty}a_n\exp\left(ik(\zeta_n-\xi)y'\right)dy'd\xi\\ &= \frac{ksgnz}{2\pi}\int\limits_{-\infty}^{\infty}\frac{c^{inf}(\xi)\exp(ik\xi y+ik|z|\gamma(\xi))}{f(\xi)}d\xi,\end{aligned} \tag{17}$$

where

$$c^{inf}(\xi)=2\sum_{n=-\infty}^{\infty}a_n\frac{\sin\left(kd(\zeta_n-\xi)\right)}{kl(\zeta_n-\xi)},$$

$$f(\xi)=1-\exp\left(ikl(\cos\phi_0-\xi)\right).$$

The integrand in (17) has singularities at the points that correspond to the cut-off frequencies of Floquet's modes. After accounting for the higher order term of uniform asymptotic presentation obtain the far field representation of the scattered field [34]

$$H_x^{s,inf}(\phi,\rho) = H_x^p(\phi,\rho) + H_x^{erfc}(\phi,\rho),$$

and

$$H_x^s(\phi,\rho) \cong H_x^p(\phi,\rho) + H_x^{erfc}(\phi,\rho) + H_x^{s,c}(\phi,\rho), \quad k\rho \to \infty,$$

where

$$\begin{aligned} H_x^p(\phi,\rho) \;=\; & \sum_q \varepsilon_q(\phi) a_q \exp(ik\rho\cos(\phi - w_q)), \quad H_x^{erfc}(\phi,\rho) = \exp\left(ik\rho - \frac{\pi i}{4}\right) \\ & \times \left[\frac{\pi}{kl}\sum_q sgn(w_q-\phi)c^{inf}(-\cos w_q) \times \exp\left(-2\,ik\rho\left(\sin\frac{\phi - w_q}{2}\right)^2\right)\right. \\ & \times \left(\frac{1+i}{\sqrt{2}} - \sqrt{2}C(\psi) - \sqrt{2}iS(\psi)\right) \\ & \left. -\frac{i}{kl}\sqrt{\frac{\pi}{2k\rho}}\left(\frac{2\,c^{inf}(-\cos\phi)}{f(-\cos\phi)}\sin\phi + \sum_q \frac{c^{inf}(-\cos w_q)}{\sin\frac{w_q-\phi}{2}}\right)\right], \end{aligned}$$

$$H_x^{s,c}(\phi,\rho) \cong \sqrt{\frac{2\pi}{k\rho}} c(-\cos\phi)\exp\left(i(k\rho - \pi/4)\right), \quad 0 < \phi < \pi.$$

Summation is over all q, which corresponds to the propagating plane waves, $|\zeta_q| < 1$.

$$\varepsilon_q(\theta) = \begin{cases} 0, & \phi < w_q, \\ 1, & \phi > w_q. \end{cases}$$

Fresnel integrals are $C(\psi) = \int_0^{\psi} \cos\left(\frac{\pi}{2}t^2\right) dt$, $S(\psi) = \int_0^{\psi} \sin\left(\frac{\pi}{2}t^2\right) dt$, where $\psi = 2\sqrt{\frac{k\rho}{\pi}}\sin\left|\frac{w_l-\phi}{2}\right|$, $w_q = \pi/2 + \arcsin\zeta_q$.

Using (8) after solving (15) and (16), the spectral function of the correction field can be calculated

$$c(\xi) \approx \frac{1}{2i}\sum_{n=0}^{\infty}\frac{1}{M}\sum_{q=1}^{M} u(t_{q,n}^{(M)})\frac{\exp(-ik\,\xi\,t_{q,n}^{(M)}) - 1}{\xi}.$$

4. Current on the strips

According to (3) and (6), function $U(y)$ equals up to a constant factor 1/m to a correction current density on the strips. From (7) it follows that $U(y) = \int_{-\infty}^{y} F(\xi)d\xi$. Then

$$U(y) \approx \pi\sum_n \frac{1}{M}\sum_q u(t_{q,n}^{(M)}).$$

The summation is over all n and q for which $t_{q,n}^{(M)} \le y$.

4.1. Numerical results

To obtain numerical results we exchange an infinite set of strips L by the bounded one $L_N = \bigcup_{m=0}^{N} (-d + lm;\ d + lm)$. This means that we assumed the correction current influenced at the finite number of strips placed near the SIG edge.

First, we should validate the presented algorithm. Convergence of the method is provided by the theorems [31]. To demonstrate the rate of convergence, we computed the root-mean-square deviations of the correction current function, $\varepsilon_M = \left|\left(J_M^c - J_{2M}^c\right)/J_{2M}^c\right|$, where $J_M^c = \int_L |U(y)|^2\, dy$; M is the number of nodes on every strip. The results are presented in Figure 2. Figure 3 shows the near field distribution at the distance $z = 0.1\lambda$ for the case of normal incidence $\phi_0 = 90^0$, $kd = \pi/2$, $kl = 7$. The results obtained using the proposed method are in very good agreement with the data of [19] obtained by the operator method.

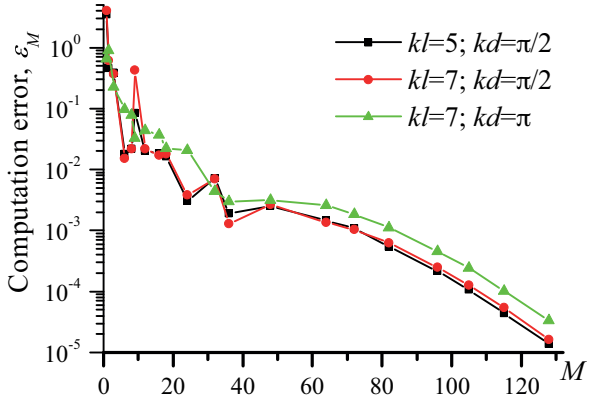

Figure 2. Computation error ε_M as a function of the number of nodes on every segment.

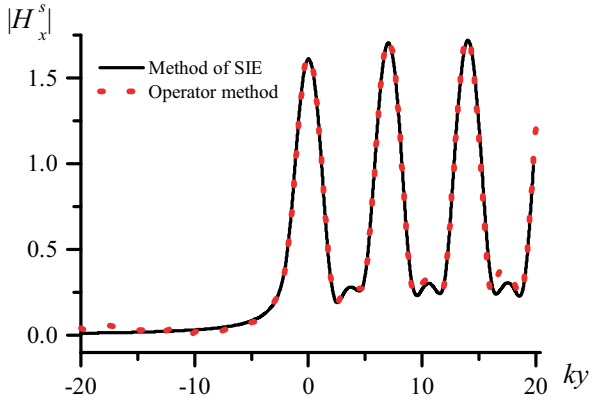

Figure 3. Field distribution for $kz = 0.628$, $kd = \pi/2$, $kl = 7$. Presented approach (solid line) and method from [19] (dotted line).

Figures 4 and 5 show the diffraction patterns $D(\phi,\rho) = \left|H_x^{erfc}(\phi,\rho) + H_x^{s,c}(\phi,\rho)\right|$ and $H_x^{s,c}(\phi,\rho)$ at distance $k\rho = 30$ for different values of period and strip width. For comparison, the Kirchhoff solution ($H_x^{s,c}(\phi,\rho) \equiv 0$) is also shown in Figure 4. We take $M = 15$ nodes on every strip, $N = 50$, and to calculate $g(y)$ we take 9 nodes and 1000 summands. Therefore, the matrix dimension is 750 $\times$ 750. Total calculation time by the method of SIE was about 45 min for Figure 4a. When we use the operator method, a nonlinear operator equation is obtained. To solve it the iterative procedure is used. Seven matrixes with dimension 1457 $\times$ 1457 each were stored in the computer memory. Total number of iterations was 3, and total calculation time by the operator method was about 55 min for Figure 4a. Thus, the operator method requires about 25 times more computer memory than the method of SIE. In the case when $kl = 2\pi$ ($l = \lambda$) we take $N = 150$. The kernel functions in the singular integral equations are calculated with an error less than 10^{-5}. The plots are normalized by the maximum value for $kd = \pi/2$, $kl = 2\pi$. The strip width $kd = \pi/2$ ($2d = \lambda/2$) and $kd = \pi$ ($2d = \lambda$) relates to the resonant region. When $kl < 2\pi$, one can observe the presence of one main lobe in the diffraction patterns. Case $kl = 2\pi$ ($l = \lambda$) corresponds to the regime of Wood's anomalies when high order propagating Floquet's modes arise. For a finite structure, this regime leads to exciting of a leaky wave. An additional lobe appears near $\phi = 0^0$. A significant increase in $H_x^{s,c}(\phi,\rho)$ especially near the directions of

propagation of Floquet's modes $\phi = 0^0$, $\phi = 90^0$, and $\phi = 180^0$ is observed in this case. The discontinuities of diffraction patterns $D(\phi, \rho)$ in the directions of propagation of Floquet's modes are present. However, the total reflected field $H_x^{ref}(\phi, \rho)$ does not contain discontinuities since the field of Floquet's modes $H_x^p(\phi, \rho)$ is added. The appearance of discontinuities for the E-polarization case was discussed in [2]. To validate the obtained results we have also presented the results obtained by the operator method as asterisks [18,19]. Good agreement is observed.

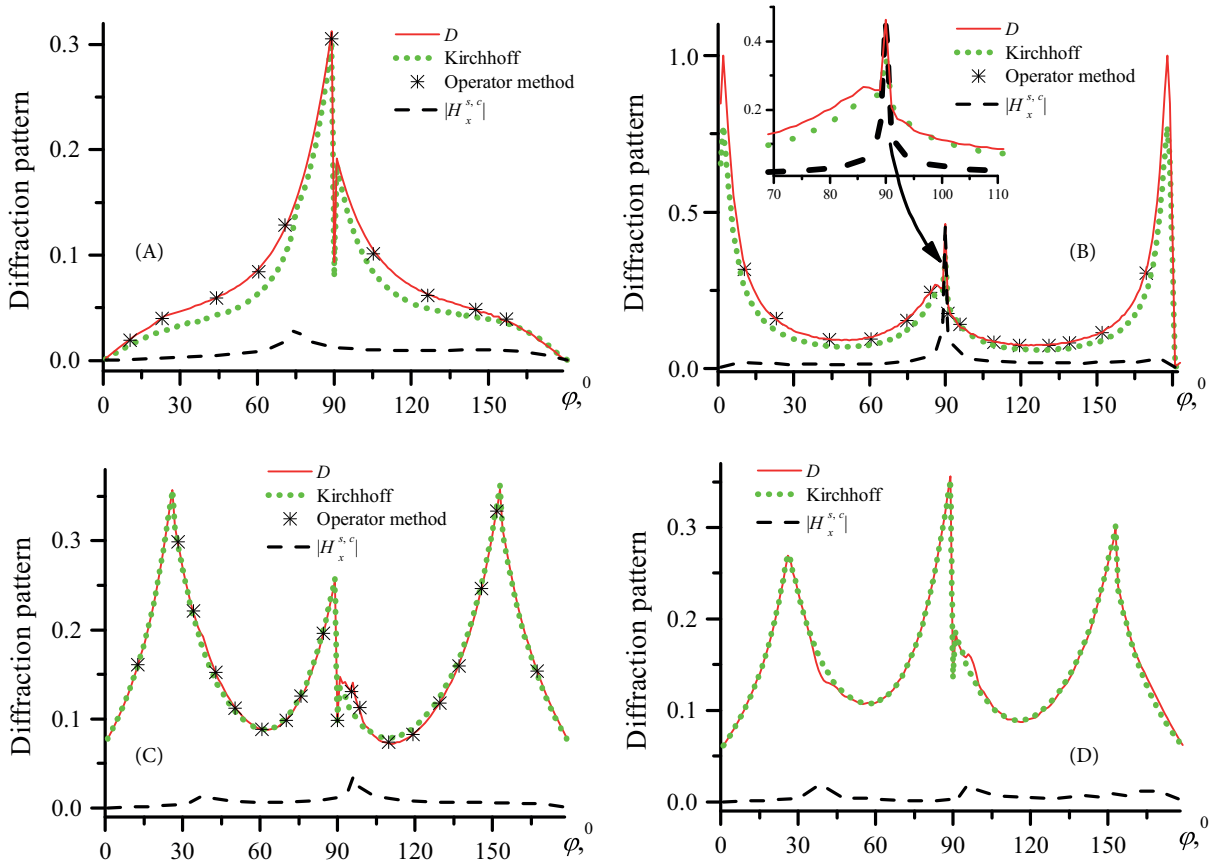

Figure 4. Diffraction patterns, $k\rho = 30$. a) $kd = \pi/2$, $kl = 5$; b) $kd = \pi/2$, $kl = 2\pi$; c) $kd = \pi/2$, $kl = 7$; d) $kd = \pi$, $kl = 7$. Results obtained by the operator method [18,19] are represented as asterisks.

Figures 6 and 7 show the field distribution $|H_x^{s,c}(y,z)|$ and $|H_x^s(y,z)|$ in the plane of the SIG $z = 0$. Field $H_x^{s,c}(y,z) = U(y)$ equals up to a constant factor to the correction current density and $H_x^s(y,z)$ equals up to a constant factor to the total current density. To obtain smooth curves we take $M = 50$. The maximum is observed near the center of the strips for $kd = \pi/2$. For $kd = \pi$ two maxima of $|H_x^{s,c}(y,z)|$ are observed for every strip. The correction current is relatively large near the end of the SIG. With the y increase the amplitude of a correction current decreases. In cases when $kl = 2\pi$, the correction current extends on a larger part of the grating. The field of the IPG $H_x^{s,inf}(y,z)$ in the center of strips, $y = lm$, is shown by a dashed line.

Let us quantify the correction current influence by the value $J^c = \int\limits_L |U(y)|^2 \, dy$. This allows us to estimate the value of the end-effect contribution [1,2]. Figure 8 shows the dependence of J^c vs. l. The strips interaction in a plane strip grating is weak, and with the increase in l it becomes negligible except for the values that

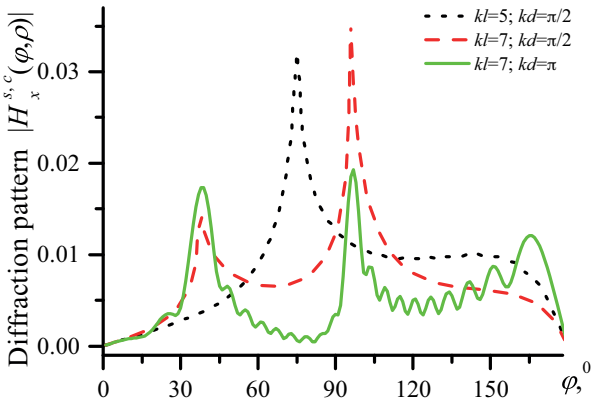

Figure 5. Diffraction patterns of correction field, $k\rho = 30$, $kl = 5$, $kd = \pi/2$ (dotted line), $kl = 7$, $kd = \pi/2$ (dashed line), $kl = 7$, $kd = \pi$ (solid line).

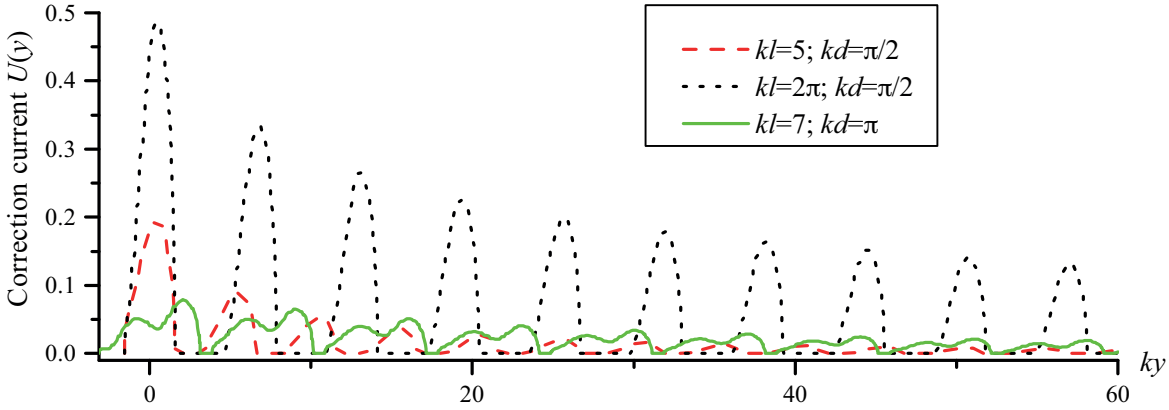

Figure 6. Field distribution $|H_x^{s,c}(y,z)|$ in the plane of the SIG, $z = 0$, for $kl = 5$, $kd = \pi/2$ (dashed line), $kl = 2\pi$, $kd = \pi/2$ (dotted line), $kl = 7$, $kd = \pi$ (solid line).

correspond to the cut-off of Floquet's modes. The significant increase in the correction current density occurs near the Wood's anomalies region, $l = m\lambda$ for $\phi_0 = 90^0$ (see also Figure 4b).

The near field around the edge of the SIG, component $Re(H_x^s(y,z))$, is shown in Figure 9. As can be seen, the two types of waves are propagating away from the grating. One of them is a plane wave that exists only in the domain $y > 0$ ($\phi > 90^0$). Another one is a cylindrical wave that is excited due to the end of the SIG. Line $y = 0$ ($\phi = 90^0$) acts as a shadow boundary.

5. Conclusions

Here, in this paper, a rigorous solution of the H-polarized plane wave diffraction by the semi-infinite periodic strip grating is obtained. The scattered field is represented as the field of currents on the infinite periodic grating and the correction field. The spectral function of the correction field as well as Fourier amplitudes of the field of infinite periodic grating is obtained from the singular integral equations with additional conditions. The Nystrom-type method of discrete singularities is used for discretization of these equations. The results are validated by comparison with those obtained by the operator method. The numerical results revealed the influence of the end of the grating. It is shown that a significant increase in the correction current density occurs near the Wood's anomalies region and correction current extends on a larger part of the grating.

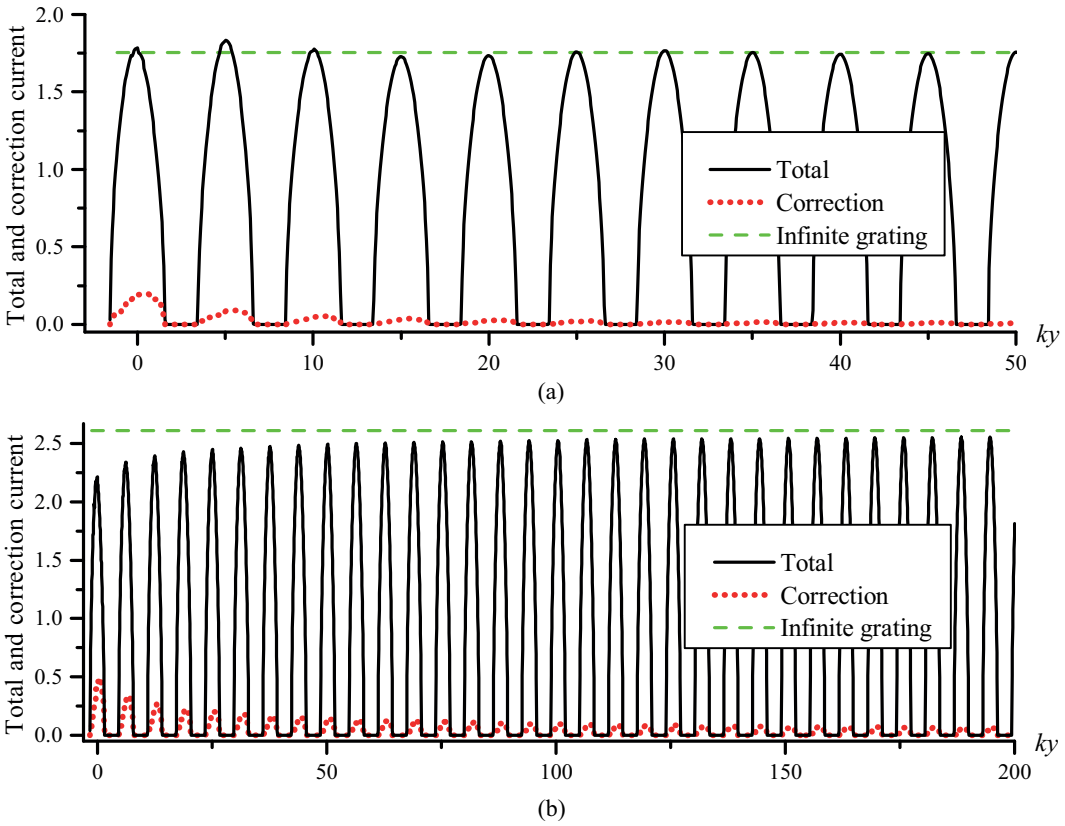

Figure 7. Field distribution $|H_x^{s,c}(y,z)|$ (dotted line), $|H_x^s(y,z)|$ (solid line), $H_x^{s,inf}(lm,z)$ (dashed line) in the plane of the SIG, $z=0$, $kd=\pi/2$. a) $kl=5$; b) $kl=2\pi$.

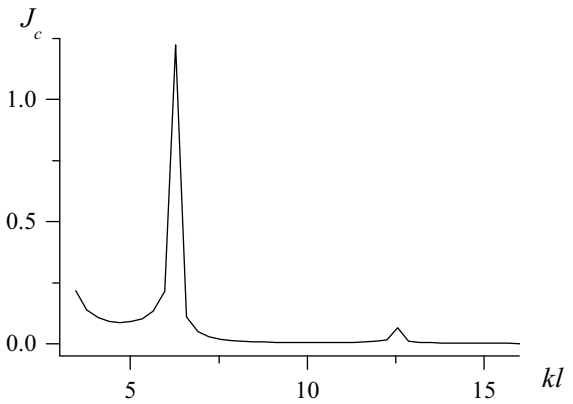

Figure 8. Correction current influence, $kd=\pi/2$.

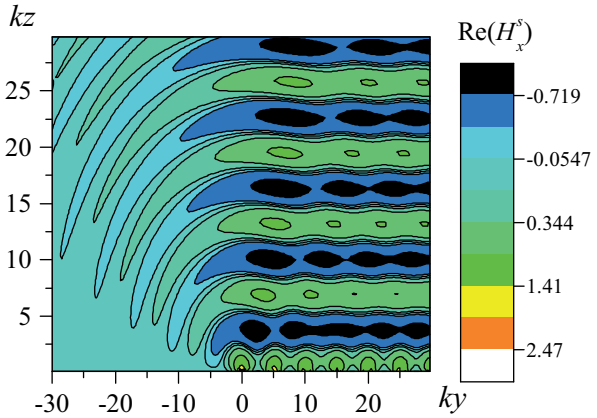

Figure 9. Field distribution $Re(H_x^s(y,z))$ for $kd=\pi/2$, $kl=5$.

References

[1] Nishimoto M, Ikuno H. Analysis of electromagnetic wave diffraction by a semi-infinite strip grating and evaluation of end-effects. Prog Electromagn Res 1999; 23: 39-58.

[2] Nishimoto M, Ikuno H. Numerical analysis of plane wave diffraction by a semi-infinite grating. T IEE Japan 2001; 121-A: 905-910.

[3] Cho YH. Arbitrarily polarized plane-wave diffraction from semi-infinite periodic grooves and its application to finite periodic grooves. Prog Electromagn Res M 2011; 18: 43-54.

[4] Savin A, Steigmann R, Bruma A. Metallic strip gratings in the sub-subwavelength regime. Sensors 2015; 14: 11786-11804.

[5] Fel'd YN. Electromagnetic wave diffraction by semi-infinite grating. J Commun Technol El+ 1958; 3: 882-889.

[6] Fel'd YN. On infinite systems of linear algebraic equations connected with problems on semi-infinite periodic structures. Doklady AN USSR 1955; 114: 257-260 (article in Russian with an abstract in English).

[7] Hills NL, Karp SN. Semi-infinite diffraction gratings–I. Commun Pur Appl Math 1965; 18: 203-233.

[8] Hills NL. Semi-infinite diffraction gratings–II, inward resonance. Commun Pur Appl Math 1965; 18: 385-395.

[9] Wasylkiwskyj W. Mutual coupling effects in semi-infinite arrays. IEEE T Antenn Propag 1973; 21: 277-285.

[10] Linton CM, Porter R, Thompson I. Scattering by a semi-infinite periodic array and the excitation of surface waves, SIAM J Appl Math 2007; 67: 1233-1258.

[11] Hadad Y, Steinberg BZ. Green's function theory for infinite and semi-infinite particle chains. Phys Rev B 2011; 84: 125402.

[12] Capolino F, Albani M. Truncation effects in a semi-infinite periodic array of thin strips: a discrete Wiener-Hopf formulation. Radio Sci 2009; 44: 1-14.

[13] Nepa P, Manara G, Armogida A. EM scattering from the edge of a semi-infinite planar strip grating using approximate boundary conditions. IEEE T Antenn Propag 2005; 53: 82-90.

[14] Caminita F, Nannetti M, Maci S. An efficient approach to the solution of a semi-infinite strip grating printed on infinite grounded slab excited by a surface wave. In: XXIX URSI General Assembly; 7–13 August 2008; Chicago, IL, USA: URSI. BPS 2.5.

[15] Kaliberda ME, Litvinenko LN, Pogarskii SA. Operator method in the analysis of electromagnetic wave diffraction by planar screens. J Commun Technol Electron 2009; 54: 975-981.

[16] Vorobyov SN, Lytvynenko LM. Electromagnetic wave diffraction by semi-infinite strip grating. IEEE T Antenn Propag 2011; 59: 2169-2177.

[17] Lytvynenko LM, Kaliberda ME, Pogarsky SA. Solution of waves transformation problem in axially symmetric structures. Frequenz 2012; 66: 17-25.

[18] Lytvynenko LM, Kaliberda ME, Pogarsky SA. Wave diffraction by semi-infinite venetian blind type grating. IEEE T Antenn Propag 2013; 61: 6120-6127.

[19] Kaliberda ME, Lytvynenko LM, Pogarsky SA. Diffraction of H-polarized electromagnetic waves by a multi-element planar semi-infinite grating. Telecommun Radio Eng+ 2015; 74: 348-357.

[20] Martin PA, Abrahams ID, Parnell WJ. One-dimensional reflection by a semi-infinite periodic row of scatterers. Wave Motion 2015; 58: 1-12.

[21] Matsushima A, Itakura T. Singular integral equation approach to plane wave diffraction by an infinite strip grating at oblique incidence. J Electromagnet Wave 1990; 4: 505-519.

[22] Matsushima A, Nakamura Y, Tomino S. Application of integral equation method to metal-plate lens structures. Prog Electromagn Res 2005; 54: 245-262.

[23] Nosich AI. The method of analytical regularization in wave scattering and eigenvalue problems: foundations and review of solutions. IEEE T Antenn Propag Mag 1999; 41: 34-49.

[24] Nosich AI. Method of analytical regularization in computational photonics. Radio Sci 2016; 51: pp. 1421-1430.

[25] Lucido M, Panariello G, Schettino F. Scattering by a zero-thickness PEC disk: a new analytically regularizing procedure based on Helmholtz decomposition and Galerkin method. Radio Sci 2017; 52: 2-14.

[26] Oğuzer T, Kuyucuoğlu F, Avgın İ. Electromagnetic scattering from layered strip geometries: the method of moments study with the sinc basis. Turk J Electr Eng & Comp Sci 2011; 19: 397-412.

[27] Shapoval OV, Sauleau R, Nosich AI. Scattering and absorption of waves by flat material strips analyzed using generalized boundary conditions and Nystrom-type algorithm. IEEE T Antenn Propag 2011; 59: 3339-3346.

[28] Tsalamengas J. Exponentially converging Nystrom's methods for systems of SIEs with applications to open/closed strip or slot-loaded 2-D structures. IEEE T Antenn Propag 2006; 54: 1549-1558.

[29] Tong MS, Chew WC. Nystrom method with edge condition for electromagnetic scattering by 2-D open structures. Prog Electromagn Res 2006; 62: 49-68.

[30] Kaliberda ME, Lytvtnenko LM, Pogarsky SA. Singular integral equations in diffraction problem by an infinite periodic strip grating with one strip removed. J Electromagnet Wave 2016; 30: 2411-2426.

[31] Gandel YV. Method of discrete singularities in electromagnetic problems. Problems of Cybernetics 1986; 124: 166-183 (article in Russian with an abstract in English).

[32] Nosich AA, Gandel YV. Numerical analysis of quasioptical multireflector antennas in 2-D with the method of discrete singularities: E-wave case. IEEE T Antenn Propag 2007; 55: 399-406.

[33] Gandel YV. Boundary-value problems for the Helmholtz equation and their discrete mathematical models. Journal of Mathematical Sciences 2010; 171: 74-88.

[34] Felsen LB, Marcuvits N. Radiation and Scattering of Waves. Englewood Cliffs, NJ, USA: Prentice-Hall Inc., 1973.